Self-powered microfluidic chips for multiplexed protein assays from whole blood†

Lidong Qin, Ophir Vermesh, Qihui Shi and James R. Heath*

Received 27th November 2008, Accepted 25th March 2009
First published as an Advance Article on the web 16th April 2009
DOI: 10.1039/b821247c

We report herein on a self-powered, self-contained microfluidic-based chip designed to separate plasma from whole blood, and then execute an assay of a multiplexed panel of plasma biomarker proteins. The power source is based upon a chemical reaction that is catalytically triggered by the push of a button on the chip. We demonstrate assays of a dozen blood-based protein biomarkers using this automated, self-contained device. This platform can potentially permit high throughput, accurate, multiplexed blood diagnostic measurements in remote locations and by minimally trained individuals.

Introduction

Blood contains the most comprehensive version of the human proteome, and as such, blood-based protein biomarkers constitute the most commonly used diagnostic material for monitoring disease and health.[1–3] The protein sandwich assay, or the enzyme-linked immunosorbent assay (ELISA),[4] is widely used for measuring protein biomarker levels. The integration of sandwich assays into microfluidic systems can permit the evaluation of diagnostic markers from small quantities of blood,[5,6] with an accompanying reduction in reagent use and fast, few-minute assay times. Most microfluidic-based assays, however, involve significant macro-accessories, such as pumps, power supplies and fluid handling systems.[7–9] These accessories, in turn, add complexity to assay execution, and significantly limit the portability and flexibility of such devices. We report here on a self-powered, self-contained microfluidic-based chip designed to separate plasma from whole blood, and then execute an assay of a multiplexed panel of plasma biomarker proteins. The power source, which is the key development reported here, pumps the blood, reagents, *etc.*, through the microfluidic channels. It is based upon a chemical reaction that is catalytically triggered by the push of a button on the chip.

Pumps for microfluidic-based chips have been reported by a number of groups.[10–13] For example, pressure sources from gas cylinders, air pumps, or syringe pumps have been utilized.[7,8] Other alternatives have included the use of electrochemical reactions to generate gas bubbles or the use of paraffin actuators to power microfluidic devices.[14–23] All of these approaches require at least some level of off-chip accessories to execute an assay. A disadvantage of these on-chip pump approaches is that they typically require an electrical power supply, and the solution flow rate is limited. The chemically-powered chip that we describe can be completely self-contained, and the reaction itself can be controlled to allow for broad control over the flow rate. We demonstrate that this can be advantageous for certain applications.

Our source of power originates from the Pt/Ag catalyzed decomposition of diluted H_2O_2 to generate oxygen (Fig. 1). Depending upon the starting H_2O_2 concentration, the O_2 reaction product expands up to 100-fold relative to the starting liquid volume.[24] H_2O_2 decomposition is spontaneous ($\Delta G^\circ = -119.2$ kJ mol^{-1}), but commercially available H_2O_2 contains stabilizing agents, and is stable until exposed to a catalyst trigger. A Pt catalyst promotes the first order decomposition of H_2O_2, with a rate that is limited by the diffusion of H_2O_2 to the catalyst surface. As shown in Fig. 1, the designed microfluidic device contains a hydrogen peroxide reservoir, which connects to the functional region of the microfluidic-based assay *via* a bridging channel. The bridge traverses the top side of the device, and thus avoids contact between the H_2O_2 reservoir and the sample chamber. The top of the device is covered with a ~2 mm thick PDMS lid, and a pinhole is fabricated into this lid for inserting Pt/Ag catalytic pin plugs to trigger the device. (Fig. 1A)

The pressure, generated by the chemical reaction, if not mediated, can be sufficient to delaminate the entire device. To avoid this problem, an empty buffer chamber is connected to the peroxide reservoir through a bottom channel. When the reaction is triggered, the generated pressure pushes the peroxide solution into the buffer chamber. The result is that the peroxide fuel level is lowered below that of the Pt/Ag catalyst pin, thus stopping O_2 generation, and preventing over- pressurization of the chip. The pressure inside the peroxide chamber then decreases as the gas drives fluid through the microfluidic channels. This raises the level of the peroxide solution in the reaction chamber so that it re-contacts the Pt/Ag pin. Balancing these two effects so as to generate a reliable and smoothly operating power source for the assay is accomplished by controlling the amount of peroxide solution, the peroxide concentration, and the pin plug size. PDMS is gas permeable, but gas transport through the PDMS does not compete with the rate of O_2 generation.

Results and discussion

The pressure generated inside the buffer chamber was monitored using a piezoelectric micro-pressure transducer

NanoSystems Biology Cancer Center(NSBCC), Kavli Nanoscience Institute, Division of Chemistry and Chemical Engineering, California Institute of Technology, Pasadena, California, 91125, USA. E-mail: heath@caltech.edu; Tel: +1 626-395-6079

† Electronic supplementary information (ESI) available: Two movies and a document for blood assay reagents. See DOI: 10.1039/b821247c

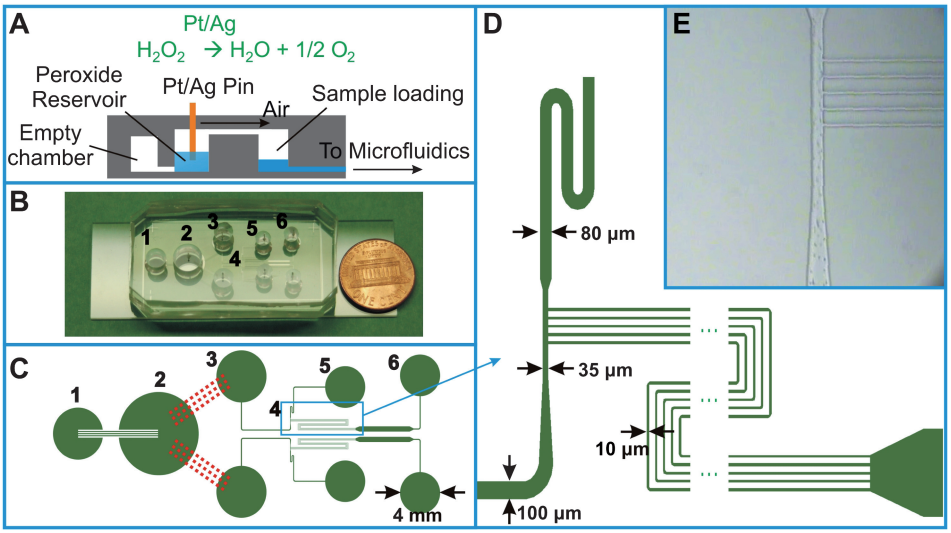

Fig. 1 Schematic design of automatic blood assay chip. (A) The configuration of the micro-pump, which is composed of H_2O_2 reservoir, Pt/Ag pin catalyst, protective chamber, and a sample loading chamber. (B) Photograph of an automated blood assay device. (C) Autocad design of the flow layer with two sets of separated whole blood assay channels. Red dash lines indicate the air bridges above the flow layer. The numbered components are the (1) empty buffer chamber, (2) H_2O_2 reservoir, (3) chamber for introducing whole blood, (4) blood skimming channels, (5) blood waste outlet, and (6), the plasma outlet. (D) An expanded view of the plasma skimming design. (E) Optical micrograph of on-chip plasma separation from whole blood.

(Endevco 8507C-15), which can monitor pressure changes with an accuracy of about 0.01 kPa. With a Pt pin size of 0.64 mm in diameter, pressure versus time plots were generated (Fig. 2). For a 6% peroxide solution, the pressure rises to 3 KPa within 1 minute of operation, stabilizes at 15 kPa, and permits more than five hours of continuous operation. This is sufficient to pump the microfluidics without damaging the PDMS device, and much more than sufficient to complete an assay. If the buffer chamber is not incorporated into the design, then the pressure will build up continuously until the device delaminates at ~60 kPa (Fig. 2, black curve). The optimized pressure and pin size, as well as the

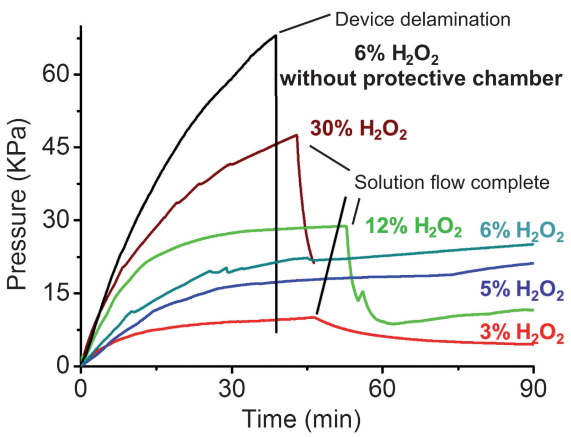

Fig. 2 Chamber pressure inside the peroxide device measured by a micro piezoelectric pressure transducer. The pressure is tuned by the H_2O_2 concentration in the automated IBBC fuel reservoir, modulated by the protective chamber. If no such protective chamber is included in the design, the increasing pressure will eventually destroy the device. Solution flow is complete when the entire solution volume in the chip has been pushed out *via* the outlets.

design of the protective chamber, permit the automated separation of plasma from whole blood, and the subsequent, rapid assay of blood proteins.

We recently reported on an (externally powered) Integrated Blood Barcode Chip (IBBC) that was designed for the on-chip separation of plasma from whole blood, followed by a multiplexed assay of blood protein biomarkers.[3] The time from fingerprick to the completion of the critical steps in those assays was less than 10 minutes. This time-scale is faster than many of the blood chemical processes that can degrade protein levels.[25] We adopted that design here as an illustrative example of a self-powered chip. Plasma is separated from whole blood into plasma skimming channels using the Zweifach-Fung effect.[26,27] The glass bottom surfaces of the plasma skimming channels are pre-patterned with ssDNA barcodes. These barcodes are converted into antibody barcodes using the DNA-encoded antibody libraries (DEAL) method.[28] Plasma protein biomarkers are captured onto individual barcode strips using specific antibody-antigen binding; each stripe within a barcode represents an assay for one protein; a complete barcode represents a full assay for a panel of, in this case, 12 protein biomarkers. The sandwich assay is completed by flowing biotinylated 2° antibodies, followed by fluorescently-labeled straptavidin.

The self-powered IBBCs reported here were fabricated using standard microfluidic device protocols. The photomask pattern of the designed flow layer (Fig. 1C) was first translated into a positive structure on a silicon wafer using SPR 220-7 photoresist. The structure was then used as a mould to form the ~8 mm 10:1 PDMS (10: 1 GE RTV 615 A & B) flow layer of the microfluidics chip. The flow and control layer channel heights were ~11 um and ~20 um respectively. The PDMS mould was punched with holes (green circles, Fig. 1C) and bonded to a glass slide that was pre-patterned with ssDNA bar codes.[3] The top PDMS layer, which contained the bridge connections between

the peroxide reservoir and sample injection chamber, was aligned with and bonded to the flow layer to form the final device (Fig. 1B). The micro-pump, sample injection, plasma skimming component, and protein assay region were all integrated into a compact package (Fig 1b). The chip was designed for two separate assays – one starting with fresh blood, the other with fresh, spiked blood to serve as a control.

A chip could be primed for an assay, and then stored at 4 °C for a week, prior to use. For the priming step, the ssDNA barcodes were first converted into antibody barcodes using ssDNA′-labeled primary antibodies. To do this, 50 μL of a 1% BSA/PBS solution was added to each sample injection chamber using a regular syringe and the solution was lightly pushed through the microfluidic region. Mixed primary antibodies, which were conjugated with ssDNA′ oligomers that were complimentary to the ones on the glass substrates (Fig. S1†), were then applied to the device and washed away. The fuel reservoir was then filled with 0.1 ml 6% H_2O_2 and a Pt pin was inserted into the top pinhole, but not deeply enough to contact the H_2O_2 fuel. At this stage, the chips could be stably stored.

In a typical assay, a fingerprick of human blood (2 μL) is collected and directly applied, *via* syringe, to the sample reservoir, where it is mixed by diffusion with 20 μL of a preloaded EDTA/BSA/PBS solution. Since human blood can constitute a safety hazard, all procedures were conducted according to safety protocols approved by the Caltech Institutional Review Board. In addition, all appropriate steps were taken to maintain the privacy and confidentiality of all participants who gave blood for the study. Two (non-catalytic) pins are used to block the blood inlet. The assay is then triggered by pushing the Pt plug into contact with the peroxide reservoir. Pressure builds up inside the device within a few seconds and drives the blood through the blood-skimming channel (Video 1, ESI†). Plasma (>99% cell-free) is skimmed into the assay channels (Fig. 1E, Video 1†). After a set time of operation, flow is stopped by raising the Pt pin. At this point, information about plasma protein levels has been recorded by the antibody barcodes. In principle, the development of the assay (with fluorescently-labeled secondary antibodies) could be automated similarly. However, for this work, the PDMS layers were simply peeled away from the glass slide, and the development and barcode reading steps were then done on the glass slide. The development step includes the addition of a single solution containing the biotinylated secondary antibodies and streptavidin-Cy5. After rinsing and drying, the developed barcode slides are read using a standard gene chip scanner (Axon Genepix 4000B), and the detected proteins appear as fluorescent bars within the barcodes (Fig. 3 and 4). Although the chip scanner is not portable, fully developed barcode assay slides may be stored for many days in ambient conditions without affecting the readout.

The off-chip powered IBBC was previously utilized for the quantitative detection of proteins in human plasma. Herein we verified on-chip detection limits for these automated IBBCs, also starting from whole human blood, for a representative protein, Interleukin-12 (IL-12). IL-12 was spiked, at various concentrations, into fresh blood from a healthy human donor, and that blood was then assayed for IL-12 using an automated IBBC, as described above (Fig. 3). For each concentration, the stripes from 10 separate barcodes that corresponded to the IL-12

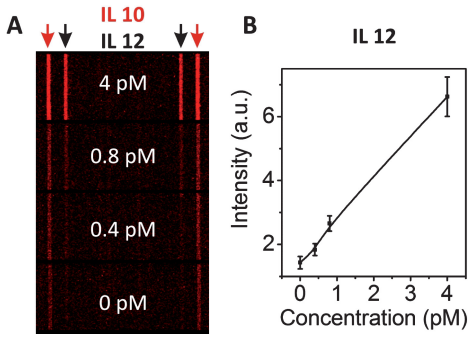

Fig. 3 Dilution curves for IL 12, as measured from spiked whole blood using an automated IBBC. (A) Barcode images for 4 different spiked concentrations of IL-12. IL-10 (indicated with red arrows) is detected in the blood. (B) Quantitation of fluorescence intensity vs. concentration in the sub-10 pM concentration region.

readout location were imaged, digitized, and averaged by ImageJ (www.rsbweb.nih.gov/ij). IL-12 exhibited a consistent trend of intensity vs. concentration with a detection limit of approximately 0.4 pM. This compares with the vendor-quoted ELISA detection sensitivity of 15 pg/ml (0.3 pM) (eBioscience). This data indicates that the automated IBBC can assay for blood proteins within a clinically relevant concentration range.[29]

As a demonstration of a multiplexed, rapid protein assay, two fingerpricks of blood from the same healthy volunteer were assayed using a 12-cytokine biomarker panel. One fingerprick was directly applied to the chip and the other was protein-spiked at a relatively high[1] concentration of 300 pg/ml. One bar within each barcode was functionalized with an ssDNA oligomer that was not complementary to any ssDNA′-labeled 1° antibody conjugates, and served as an alignment marker and a negative control.[30–32] Both the non-spiked and spiked fingerprick blood samples were assayed simultaneously on the same chip, and were then read out simultaneously (Fig. 4). The spiked human blood

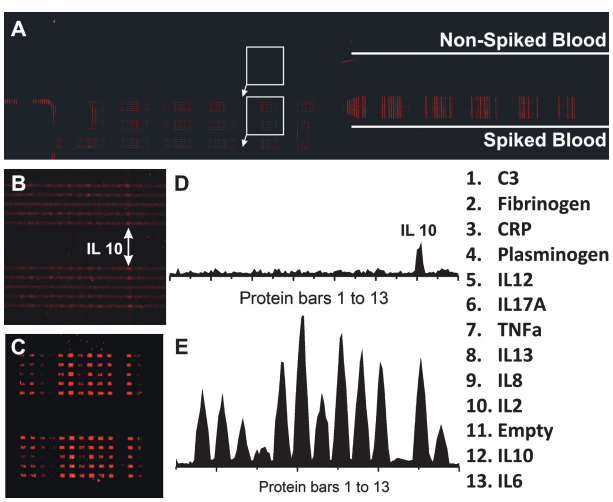

Fig. 4 Human blood protein identification using an automated IBBC. (A) Overview: a scanning fluorescent image of non-spiked blood (upper) and spiked blood (bottom). (B) Zoomed-in view of non-spiked blood and (C) spiked blood. (D) Line-signal profile of non-spiked blood (amplified three times) and (E) spiked blood. The investigated 12 proteins and their corresponding barcode positions are listed on the right.

sample shows clearly all 12 protein bars, as well as the (blank) control (bar #11). However, for the non-spiked blood sample, only IL-10 was detected (Fig. 3B and D) with signal to background ratio of 3.5 (standard deviation = 0.6). This detected level of IL-10 in healthy human blood is reasonable.[33–35]

Assays carried out under conditions of sufficiently high plasma flow rates are limited only by the kinetics of antibody/protein binding, and so should only take a few minutes.[32] We explored the kinetics of our automated blood assays, carried out at various flow rates, in an effort to identify the minimum time required per assay. (For this purpose, the 6 plasma skimming channels within a single fingerprick measurement device were designed with different channel widths (Fig. 5), and hence different flow rates within an otherwise identical assay. The sub-channels were elongated to realize the flow speed differences between channels – a design modifcation that did not detrimentally influence the plasma separation process.[36] After a 2 minute flow period, protein levels recorded in the six individual channels are different: the widest (fastest-flow rate) channel exhibited higher signals levels, as would be expected.[37,38] However, for flow times of 5 minutes, the measured signals in all of the skimming channels was saturated and yielded identical signal levels (Fig. 5C and E). Fluid flow in microfluidic channels has a parabolic flow profile,[32] with low flow near the channel walls and high flow in the channel center. For unsaturated assays (Fig 5D), this variance in flow rate leads to a parabolic- shaped signal, peaked in the region of the barcode that corresponded to the center of the channel. For saturated assays, this effect is gone. This study implies that the time from fingerprick to completion of the critical assay steps can be reduced to 5 minutes without loss in sensitivity. We have used 20 of these automated chips for 5 minute assays of protein biomarkers from fingerpricks of human blood, and all have produced reliable results. The detection sensitivity and accuracy is limited by the barcode-patterning[35] and the antibodies, but not by the automation.

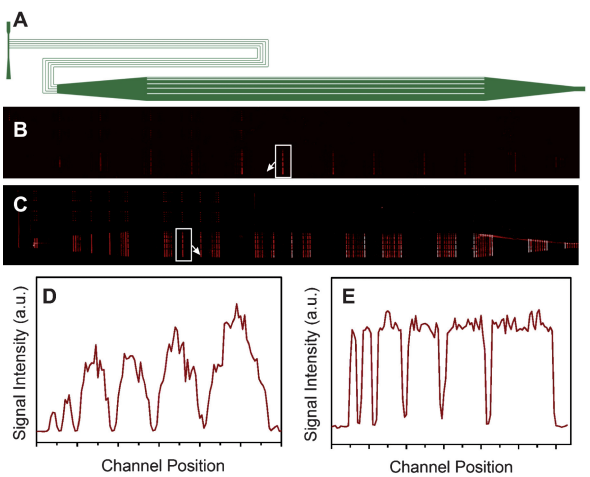

Fig. 5 Flow speed-dependent study of spiked human blood. (A) Channel design of varying speed plasma channel. (B) Scanning fluorescent image of a 2-minute blood assay and (C) a 5-minute assay. (D) and (E) are line profiles of image B and C in the squared region and in the vertical direction.

Conclusions

The design of an automatic microfluidic platform is reported, and applied towards the demonstration of rapid blood protein assays from whole blood. H_2O_2 fuel is integrated on-chip, and assays of a dozen blood-based protein biomarkers are initiated with a simple push-button operation. This simple "plug-and-play" platform can potentially permit high throughput, accurate, multiplexed blood diagnostic measurements in remote locations and by minimally trained individuals.

Acknowledgements

We would like to thank Dr. Rong Fan, Habib Ahmad, and Ke Xu for helpful discussions, and for providing assistance with certain aspects of device fabrication. This work was funded by the National Cancer Institute grant no. 5U54 CA119347 (J.R.H., P.I.), by the Institute for Collaborative Biotechnologies through grant DAAD19-03-D-0004 from the US Army Research Office, and also by the Jean Perkins Foundation.

References

1 N. L. Anderson and N. G. Anderson, *Molecular & Cellular Proteomics*, 2002, **1**, 845–867.
2 L. A. Liotta, M. Ferrari and E. Petricoin, *Nature*, 2003, **425**, 905.
3 R. Fan, O. Vermesh, A. Srivastava, B. K. H. Yen, L. Qin, H. Ahmad, G. A. Kwong, C. C. Liu, J. Gould, L. Hood and J. R. Heath, *Nat Biotech*, 2008, **26**, 1373–1378.
4 E. Engvall and P. Perlmann, *Immunochemistry*, 1971, **8**, 871–874.
5 T. G. Henares, F. Mizutani and H. Hisamoto, *Analytica Chimica Acta*, 2008, **611**, 17–30.
6 J. H. Cho, S. M. Han, E. H. Paek, I. H. Cho and S. H. Paek, *Anal. Chem.*, 2006, **78**, 793–800.
7 P. S. Dittrich, K. Tachikawa and A. Manz, *Analytical Chemistry*, 2006, **78**, 3887–3907.
8 T. Thorsen, S. J. Maerkl and S. R. Quake, *Science*, 2002, **298**, 580–584.
9 J. Gao, J. Xu, L. E. Locascio and C. S. Lee, *Anal. Chem.*, 2001, **73**, 2648–2655.
10 K. Smistrup and H. A. Stone, *Physics of Fluids*, 2007, **19**, 063101/063101–063101/063109.
11 P. Garstecki, M. J. Fuerstman, M. A. Fischbach, S. K. Sia and G. M. Whitesides, *Lab on a Chip*, 2006, **6**, 207–212.
12 I. D. Johnston, J. B. Davis, R. Richter, G. I. Herbert and M. C. Tracey, *Analyst*, 2004, **129**, 829–834.
13 G. M. Walker and D. J. Beebe, *Lab on a Chip*, 2002, **2**, 131–134.
14 P. Selvaganapathy, E. T. Carlen and C. H. Mastrangelo, *Sensors and Actuators, A: Physical*, 2003, **A104**, 275–282.
15 R. H. Liu, J. Bonanno, J. Yang, R. Lenigk and P. Grodzinski, *Sensors and Actuators, B: Chemical*, 2004, **B98**, 328–336.
16 L. Yobas, K. C. Tang, S. E. Yong and E. K. Z. Ong, *Lab on a Chip*, 2008, **8**, 660–662.
17 T. J. Pappas and L. A. Holland, *Sensors and Actuators, B: Chemical*, 2008, **B128**, 427–434.
18 D. B. Weibel, A. C. Siegel, A. Lee, A. H. George and G. M. Whitesides, *Lab on a Chip*, 2007, **7**, 1832–1836.
19 C. H. Wu, J. K. Chen and R. J. Yang, *Microfluidics and Nanofluidics*, 2007, **3**, 485–494.
20 D. Lastochkin, R. Zhou, P. Wang, Y. Ben and H. C. Chang, *Journal of Applied Physics*, 2004, **96**, 1730–1733.
21 J. Xie, Y. Miao, J. Shih, Q. He, J. Liu, Y. C. Tai and T. D. Lee, *Analytical Chemistry*, 2004, **76**, 3756–3763.
22 J. W. Munyan, H. V. Fuentes, M. Draper, R. T. Kelly and A. T. Woolley, *Lab on a Chip*, 2003, **3**, 217–220.
23 S. Liu, Q. Pu and J. J. Lu, *Journal of Chromatography, A*, 2003, **1013**, 57–64.
24 P. A. Giguère, B. G. Morissette, A. W. Olmos and O. Knop, *Can. J. Chem.*, 1955, **33**, 804–820.

25 S. Yang, A. Undar and J. D. Zahn, *Lab on a Chip*, 2006, **6**, 871–880.
26 K. Svanes and B. W. Zweifach, *Microvascular Research*, 1968, **1**, 210–220.
27 Y. C. Fung, *Microvasc. Res.*, 1973, **5**, 34–38.
28 R. C. Bailey, G. A. Kwong, C. G. Radu, O. N. Witte and J. R. Heath, *Journal of the American Chemical Society*, 2007, **129**, 1959–1967.
29 L. Romani, P. Puccetti and F. Bistoni, *Clin. Microbiol. Rev.*, 1997, **10**, 611–636.
30 B. Schweitzer, S. Roberts, B. Grimwade, W. P. Shao, M. J. Wang, Q. Fu, Q. P. Shu, I. Laroche, Z. M. Zhou, V. T. Tchernev, J. Christiansen, M. Velleca and S. F. Kingsmore, *Nature Biotechnology*, 2002, **20**, 359–365.
31 W. W. Lin and M. Karin, *Journal of Clinical Investigation*, 2007, **117**, 1175–1183.
32 M. Zimmermann, E. Delamarche, M. Wolf and P. Hunziker, *Biomedical Microdevices*, 2005, **7**, 99–110.
33 J. Karcher, C. Reisser, V. Daniel and C. Herold-Mende, *HNO*, 1999, **47**, 879–884.
34 M. Kupczyk, I. Kupryae-Lipinska, M. Bocheuska-Marciniak, P. Gorski and P. Kuna, *Allergy*, 2007, **62**, 248–248.
35 M. Navarrete, A. Palacios, M. J. Cruz, A. Blanco, I. Caragol and A. Lopez, *Blood*, 2006, **108**, 227B–227B.
36 D. J. Beebe, G. A. Mensing and G. M. Walker, *Annual Review of Biomedical Engineering*, 2002, **4**, 261–286.
37 O. Hofmann, G. Voirin, P. Niedermann and A. Manz, *Anal. Chem.*, 2002, **74**, 5243–5250.
38 V. G. Levich, *Physiochemical Hydrodynamics*, Prentice Hall, Englewood Cliffs, NJ, 1962.

